The Journal of Immunology

Porphyromonas gingivalis Promotes Immunoevasion of Oral Cancer by Protecting Cancer from Macrophage Attack

Shiyu Liu, Xuedong Zhou, Xian Peng, Mingyun Li, Biao Ren, Guo Cheng and Lei Cheng

J Immunol 2020; 205:282-289; Prepublished online 29 May 2020;
doi: 10.4049/jimmunol.1901138
http://www.jimmunol.org/content/205/1/282

The Journal of Immunology is published twice each month by
The American Association of Immunologists, Inc.,
1451 Rockville Pike, Suite 650, Rockville, MD 20852

Print ISSN: 0022-1767 Online ISSN: 1550-6606.

Porphyromonas gingivalis Promotes Immunoevasion of Oral Cancer by Protecting Cancer from Macrophage Attack

Shiyu Liu,*,† Xuedong Zhou,*,†,‡ Xian Peng,*,‡ Mingyun Li,*,‡ Biao Ren,*,‡ Guo Cheng,§ and Lei Cheng*,†,‡

The relationship of *Porphyromonas gingivalis* and oral squamous cell carcinoma (OSCC) has been studied for several years. Previous studies have focused on the direct effect of *P. gingivalis* on the activities of primary epithelial cells and OSCC cells. However, the immune system is responsible for mediating cancer development, whether *P. gingivalis* can affect oral cancer immunity has seldom been explored to date. In this study, we investigated the role of *P. gingivalis* in the immunoevasion of OSCC. We evaluated the effect of *P. gingivalis* on the phagocytosis of Cal-27 cells (OSCC cell line) by bone marrow–derived macrophages in vitro and studied the effect of *P. gingivalis* on the growth of OSCC and the polarization of tumor-associated macrophages in vivo. We found that *P. gingivalis* was able to inhibit the phagocytosis of Cal-27 cells by macrophages, and membrane-component molecules of *P. gingivalis*, such as proteins, were speculated to be the effector components. In addition, sustained infection with antibiotics-inactivated *P. gingivalis* promoted OSCC growth in mice and induced the polarization of macrophages into M2 tumor-associated macrophages, which mainly display protumor properties. Transcriptome analysis and quantitative RT-PCR revealed that *P. gingivalis* infection upregulated the expression of genes encoding protumor molecules in Cal-27 cells (*suprabasin*, *IL-1R2*, and *CD47*) and in macrophages (*IL-1α*, *CCL-3*, and *CCL-5*). Our in vitro and in vivo data suggest that *P. gingivalis* can promote immunoevasion of oral cancer by protecting cancer from macrophage attack. To our knowledge, the present study reveals a novel mechanism by which *P. gingivalis* promotes OSCC development. *The Journal of Immunology*, 2020, 205: 282–289.

Oral cancer is the eighth most prevalent cancer worldwide, and more than 90% of oral cancers are oral squamous cell carcinoma (OSCC) (1, 2). According to the global cancer statistics, ∼354,864 new cases and 177,384 deaths from oral cavity cancer were estimated in 2018 worldwide (3), and the 5-y survival rates for individuals with oral cancer are <50% (4). In addition, OSCC has a high chance for recurrence and metastasis, and patients who survive the first occurrence of oral cancer are at a higher risk of developing a second primary oral cancer. OSCC recurrence rates can range between 32.7 and 44.9% (5, 6). Therefore, exploring OSCC pathogenesis is critical for ensuring better prevention and improving patients' survival.

Accumulated evidence indicates that chronic periodontitis is a risk factor for oral cancer (7–9). Further, *Porphyromonas gingivalis*, a major opportunistic pathogen responsible for chronic periodontitis, may be an important mediator for the development of OSCC (10). Strong association between *P. gingivalis* and OSCC has been found in clinical investigations (11, 12). We collected more clinical OSCC samples, and the result showed that the *Porphyromonas* species was found in a higher proportion in tumor inner areas than on the tumor surface (Supplemental Fig. 1). Numerous studies have revealed the mechanisms by which *P. gingivalis* promotes oral carcinogenesis and cancer development; *P. gingivalis* was reported to inhibit programmed cell death or apoptosis in primary gingival epithelial cells (13–15), accelerate gingival epithelial cell proliferation (16, 17), promote metastatic dissemination and invasion of OSCC cells (18), and induce chronic inflammation, which is anticipated to be a potential pathway in bacteria contributing to carcinogenesis (19). However, these studies mainly focused on the direct effect of *P. gingivalis* on the activities of primary epithelial and OSCC cells in vitro. The immune system is responsible for

*State Key Laboratory of Oral Diseases, Sichuan University, Chengdu 610041, China; †Department of Cariology and Endodontics, West China Hospital of Stomatology, Sichuan University, Chengdu 610041, China; ‡National Clinical Research Center for Oral Diseases, Sichuan University, Chengdu 610041, China; §Laboratory of Molecular Translational Medicine, Centre for Translational Medicine, Key Laboratory of Birth Defects and Related Diseases of Women and Children, Ministry of Education, West China Second University Hospital, Sichuan University, Chengdu, Sichuan 610017, China

ORCIDs: 0000-0003-4215-2873 (B.R.); 0000-0002-2762-4740 (L.C.).

Received for publication September 20, 2019. Accepted for publication April 21, 2020.

This work was supported by National Natural Science Foundation of China Grants 81372889 (to L.C.) and 81430011 (to X.Z.), Science and Technology Department of Sichuan Province, China Youth Grant 2017JQ0028 (to L.C.); Innovative Research of Sichuan (to L.C.); and the Graduate Student's Research and Innovation Fund of Sichuan University (to S.L.).

S.L. contributed to conception, design, acquisition, analysis, interpretation of data, and drafted and critically revised the manuscript. X.Z. contributed to conception and critically revised the manuscript for important intellectual content. X.P., M.L., and B.R. contributed to data interpretation, and critically revised the manuscript for important intellectual content. G.C. and L.C. contributed to conception, design, data interpretation, and critically revised the manuscript for important intellectual content. All authors gave their final approval and agree to be accountable for all aspects of the work.

Raw transcriptome reads data presented in this article have been submitted to the National Center for Biotechnology Information Sequence Read Archive (https://www.ncbi.nlm.nih.gov) under accession numbers PRJNA552947 and PRJNA604716.

Address correspondence and reprint requests to Dr. Guo Cheng or Dr. Lei Cheng, West China School of Public Health, Sichuan University, Chengdu 610041, China (G.C.) or State Key Laboratory of Oral Diseases, West China Hospital of Stomatology, Sichuan University, No.14, Section 3, Renmin South Road, Chengdu 610041, China (L.C.). E-mail addresses: gcheng@scu.edu.cn (G.C.) or chenglei@scu.edu.cn (L.C.)

The online version of this article contains supplemental material.

Abbreviations used in this article: MHC II, MHC class II; OSCC, oral squamous cell carcinoma; PS, penicillin-streptomycin antibiotic mixture; qRT-PCR, quantitative RT-PCR; RNA-seq, RNA sequencing; TAM, tumor-associated macrophage.

mediating cancer development in immunocompetent hosts (20), whereas the initiation and perpetuation of cancer undergo the evasion of immune system (21). Few studies have focused on the role of *P. gingivalis* in oral cancer immunity.

Tumor microenvironment contains various immune cells, including macrophages, neutrophils, myeloid-derived suppressor cells, NK cells, dendritic cells, mast cells, and adaptive immune cells (T and B lymphocytes) (22). Among the diverse immune cells, macrophages play a major role in the recognition and clearance of cancer cells (23). Avoiding phagocytosis by tumor-associated macrophages (TAMs) is needed for the growth and metastasis of solid tumors (24), and programmed cell removal by macrophages can regulate cancer cell survival (25). Many studies have evaluated the role of *P. gingivalis* in the physiological activities of macrophages (26–28); however, whether these activities affect the ability of macrophages to attack cancer cells is seldom explored to date. Therefore, given the importance of macrophages in cancer immunity, we aimed at exploring the impact of *P. gingivalis* on macrophages mediating OSCC development.

Materials and Methods

Bacterial strains, cell lines, and growth conditions

P. gingivalis ATCC 33277 was anaerobically cultured in brain heart infusion broth (Difco, Sparks, MD) containing defibrinated blood of sheep (5%), hemin (0.5%), and vitamin K (0.1%) at 37°C (90% N_2, 5% H_2, 5% CO_2). Bacterial cells were precultured overnight and adjusted to a concentration of 2×10^8 CFU/ml.

OSCC cell line of Cal-27 was cultured in high-glucose DMEM (HyClone, Logan, UT) containing 10% FBS (Life Technologies, Waltham, MA) and 1% penicillin-streptomycin antibiotic mixture (PS; HyClone). Bone marrow–derived macrophages from BALB/c mice aged 5–6 wk were cultured in IMDM (HyClone) containing 10% FBS and 1% PS. An M-CSF (PeproTech) was used for stimulating the differentiation of monocytes into macrophages. Cells were cultured in an incubator with 5% CO_2 and 95% air at 37°C.

Inactivation of P. gingivalis

Antibiotic-mediated inactivation and heat inactivation were used in the current study. *P. gingivalis* was incubated in IMDM containing 10% PS for 2 h at 37°C or incubated in PBS for 2 h at 80°C to induce cell death. The dead cells were centrifugated and resuspended in IMDM with 2% heat-inactivated FBS when needed.

Phagocytosis assay (2 h)

In a flow cytometry tube, 2×10^8 CFU of living or inactivated *P. gingivalis* was incubated with 2×10^6 CFSE (Thermo Fisher Scientific), labeled Cal-27 cells, and 10 μg/ml anti-CD47 (B6H12; Abcam) at 37°C for 2 h. Following this, 2×10^6 macrophages were added to the medium to phagocytose tumor cells. All cells were suspended in IMDM with 2% heat-inactivated FBS. After incubation for another 2 h, macrophages were stained with allophycocyanin anti-mouse F4/80 (BioLegend), according to the manufacturer's protocol. Phagocytosis was evaluated by flow cytometry (Cytomics FC 500; Beckman Coulter) via the detection of $CFSE^+$ macrophages.

Phagocytosis assay (16 h)

In a 24-well plate, 2.5×10^5 Cal-27 cells and 2.5×10^5 macrophages were infected with inactivated *P. gingivalis* at a multiplicity of infection of 100:1 and suspended in DMEM containing 10% heat-inactivated FBS at 37°C. Anti-CD47 (10 μg/ml) was also added. After incubation overnight (~16 h), cells at the bottom of the plate were photographed using an inverted microscope (ECLIPSE Ti; Nikon, Tokyo, Japan) and were then collected into a flow cytometry tube. The cells were successively stained with the CFSE dye and allophycocyanin anti-mouse F4/80. After dyeing, 1×10^5 unlabeled Cal-27 cells were added to each tube. Phagocytosis was then evaluated by flow cytometry by determining the ratio of $CFSE^+$ Cal-27 cells to unlabeled cells.

The s.c. transplantation of OSCC in mice

Twenty-four specific pathogen-free female NOD-SCID mice, aged 5 wk, were randomly divided into four groups (six mice per group). The mice were s.c. injected with 2×10^6 Cal-27 cells suspended in 100 μl DMEM. After 1 wk, the mice were infected with 100 μl of antibiotics-inactivated *P. gingivalis* (OD_{600} = 1) suspended in physiological saline near two tumor sites or were i.p. injected with 100 μg of anti-CD47 three times a week. The tumor volume was measured at the treatment time points of day 14 and 18. *P. gingivalis* was incubated in IMDM containing 10% PS overnight for the in vivo experiments in the current study.

Role of *P. gingivalis* on TAM polarization was also evaluated. For this, 5-wk-old female NOD-SCID mice were randomly divided into two groups (five mice per group). The mice were s.c. injected with 2×10^6 GFP^+ Cal-27 cells. Two weeks later, mice were infected with 100 μl of antibiotics-inactivated *P. gingivalis* (OD_{600} = 1) near two different tumor sites three times a week. The animals were killed at the treatment time point of days 7 and 14 postinfection, and tumors were aseptically dissected and processed for TAMs polarization analysis. Briefly, the tumors were shred and incubated in medium 199 (HyClone) containing with 50 μg/ml liberase (Liberase TM; Roche Diagnostics) for 4 h at 37°C. Single cells were obtained using a 70-μm filter and transported into a flow cytometry tube. The cells were then stained with PE anti-mouse MHC class II (MHC II; Thermo Fisher Scientific), allophycocyanin anti-mouse F4/80 (BioLegend), and PE/Cy7 anti-mouse CD206 (BioLegend), according to the manufacturer's protocol. GFP^- $F4/80^+$ cells were gated as TAMs by flow cytometry, and the TAM polarization was evaluated by detecting MHC II and CD206.

All animal study procedures were approved by the ethics committee of West China School of Medicine, Sichuan University (2018105A), and all experiments were performed according to the National Institutes of Health Guide for the Care and Use of Laboratory Animals.

Transcriptome analysis of P. gingivalis*–infected Cal-27 cells and macrophages by RNA sequencing*

In a flow cytometry tube, 2×10^8 CFU of antibiotics-inactivated *P. gingivalis* was incubated with 2×10^6 Cal-27 cells or macrophages for 2 and 16 h at 37°C. The cells were then collected by centrifugation at 1000 rpm for 5 min. Total RNA isolation was then performed following the instructions provided with TRIzol reagent (Invitrogen, Carlsbad, CA). RNA quality and concentration were measured using a NanoDrop 2000 (Thermo Fisher Scientific), and RNA integrity was assessed using a Bioanalyzer 2100 System (Agilent Technologies). rRNA was deleted using a Ribo-Zero rRNA Removal Kit (Illumina) and RNA fragmentation was performed using divalent cations in an Illumina proprietary fragmentation buffer.

Random oligonucleotides and SuperScript III were used to synthesize the first-strand cDNA, followed by DNA polymerase I and RNase H for the synthesis of the second-strand cDNA. The remaining overhangs were converted to blunt ends through exonuclease/polymerase treatment, and the enzymes were then removed. After adenylation of the 3′ ends of the DNA fragments, Illumina PE adapter oligonucleotides were ligated to prepare for hybridization. cDNA fragments of the preferred 300 bp length were purified using the AMPure XP System (Beckman Coulter). DNA fragments with ligated adaptor molecules on both ends were selectively enriched using Illumina PCR Primer Cocktail in a 15-cycle PCR. Products

Table I. Primers used in the study

Designation		Sequences
Primers for Cal-27		
18S	F	5′-GGAGTATGGTTGCAAAGCTGA-3′
	R	5′-ATCTGTCAATCCTGTCCGTGT-3′
CD47	F	5′-AGAAGGTGAAACGATCATCGAGC-3′
	R	5′-CTCATCCATACCACCGGATCT-3′
IL-1R2	F	5′-GATTCAGGACATTACTATTGCG-3′
	R	5′-CTGGGATCCCAAGTCTACTTCC-3′
Suprabasin	F	5′-CAGGCTGGAAAGGAAGTGGAGA-3′
	R	5′-CTTGATGGCTGGAAGATCCGCT-3′
Primers for Macrophages		
18S	F	5′-CTTAGAGGGACAAGTGGCG-3′
	R	5′-ACGCTGAGCCAGTCAGTGTA-3′
IL-1α	F	5′-CAGTTCTGCCATTGACCATC-3′
	R	5′-TCTCACTGAAACTCAGCCGT-3′
CCL3	F	5′-TGTACCATGACACTCTGCAAC-3′
	R	5′-CAACGATGAATTGGCGTGGAA-3′
CCL5	F	5′-TTTGCCTACCTCTCCCTCG-3′
	R	5′-CGACTGCAAGATTGGAGCACT-3′

F, forward; R, reverse.

were purified (AMPure XP System) and quantified following the Agilent high-sensitivity DNA assay on a Bioanalyzer 2100 System (Agilent). Finally, the sequencing library was sequenced on a Hiseq platform (Illumina; Shanghai Personal Biotechnology).

Raw data (raw reads) were estimated in the FASTQ format. After filtration of low quality reads and reads containing adapters or poly-*N*, high-quality reads were aligned against the Cal-27 cell reference genome (http://asia.ensembl.org/Homo_sapiens/Info/Index) and macrophage reference genome (http://asia.ensembl.org/Mus_musculus/Info/Index) using Bowtie2 (http://bowtie-bio.sourceforge.net/index.shtml), and gene expressions were quantified using HTSeq 0.6.1p2 (http://htseq.readthedocs.io/). The values for reads per kilo base per million reads were calculated to normalize the expression values.

After RNA sequencing (RNA-seq), the differentially expressed genes were analyzed using DESeq (version 1.18.0) based on p values <0.05. Raw transcriptome reads reported in this paper have been deposited in the National Center for Biotechnology Information Sequence Read Archive under accession numbers PRJNA552947 (https://www.ncbi.nlm.nih.gov/sra/PRJNA552947) and PRJNA604716 (https://www.ncbi.nlm.nih.gov/sra/PRJNA604716).

Validation of differentially expressed genes by quantitative real-time PCR

To assess the reliability of RNA-seq, we performed quantitative RT-PCR (qRT-PCR) for several selected genes (Cal-27: *cd47*, *il-1r2*, and *suprabasin*; macrophages: *il-1α*, *ccl-3*, and *ccl5*). Cal-27 cells and macrophages were stimulated by antibiotics-inactivated *P. gingivalis* for 16 h at 37°C. Cells were then collected, and total RNA was isolated following the instructions provided with the TRIzol reagent (Invitrogen). RNA quality and purity were determined using a NanoDrop 2000 Spectrophotometer (Thermo Fisher Scientific, Waltham, MA). cDNA was then synthesized using a PrimeScript RT Reagent Kit with gDNA Eraser (Takara Clontech, Shiga, Japan), according to the manufacturer's instructions. Quantitative real-time PCR was performed using LightCycler-480 (Roche Diagnostics, Bromma, Sweden) with TB Green Reagent (Takara, Dalian, China), following the manufacturer's instructions. A 20-μl mixture of 10 μl of TB Green qPCR Mix (Takara), 1.6 μl of PCR primer mix, 2 μl of diluted template cDNA, and 6.4 μl of deionized distilled water was processed for RT-PCR. The relative fold changes ($2^{-\Delta\Delta Ct}$) were normalized to 18S expression. The PCR primers used in the study are listed in Table I.

Statistical analysis

Phagocytosis experiments were independently repeated thrice. Comparisons between groups during tumor volume analysis were made by ANOVA. Comparisons between groups were analyzed by unpaired t test for TAMs polarization analysis and qRT-PCR assay. The data are presented as mean ± SD, and the results were considered statistically significant at a p value < 0.05.

Results

P. gingivalis *inhibited macrophages from phagocytizing Cal-27 cells*

Macrophages play an important role in the clearance of foreign, aged, and transformed cells given its function of recognition and

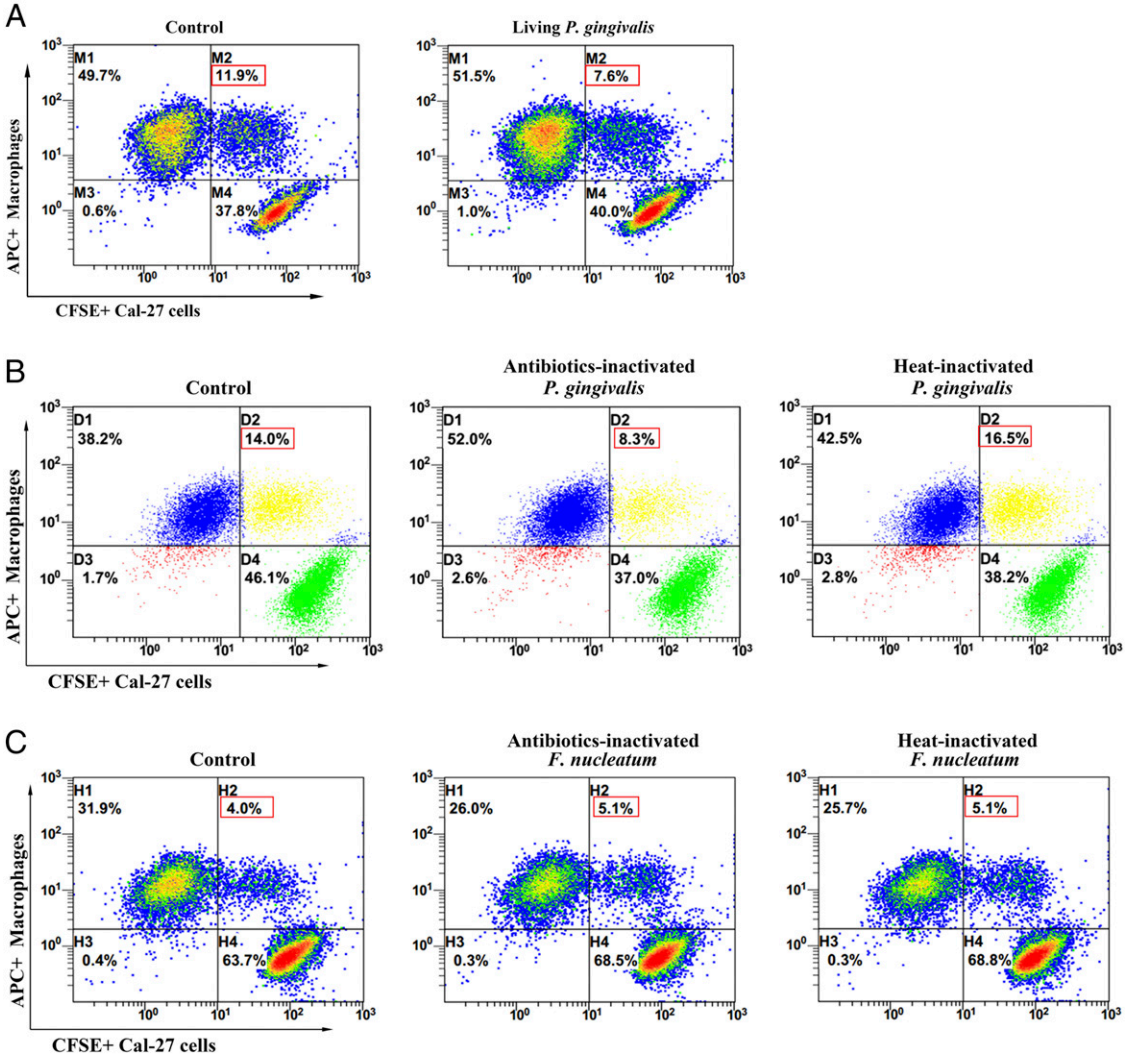

FIGURE 1. Effect of *P. gingivalis* on macrophages phagocytizing Cal-27 cells for 2 h. (**A**) Phagocytosis of Cal-27 cells by macrophages after living *P. gingivalis* treatment. (**B**) Phagocytosis of Cal-27 cells by macrophages after inactivated *P. gingivalis* treatment. (**C**) Phagocytosis of Cal-27 cells by macrophages after inactivated *F. nucleatum* treatment. The numbers in red boxes represent the proportion of macrophages that phagocytized Cal-27 cells.

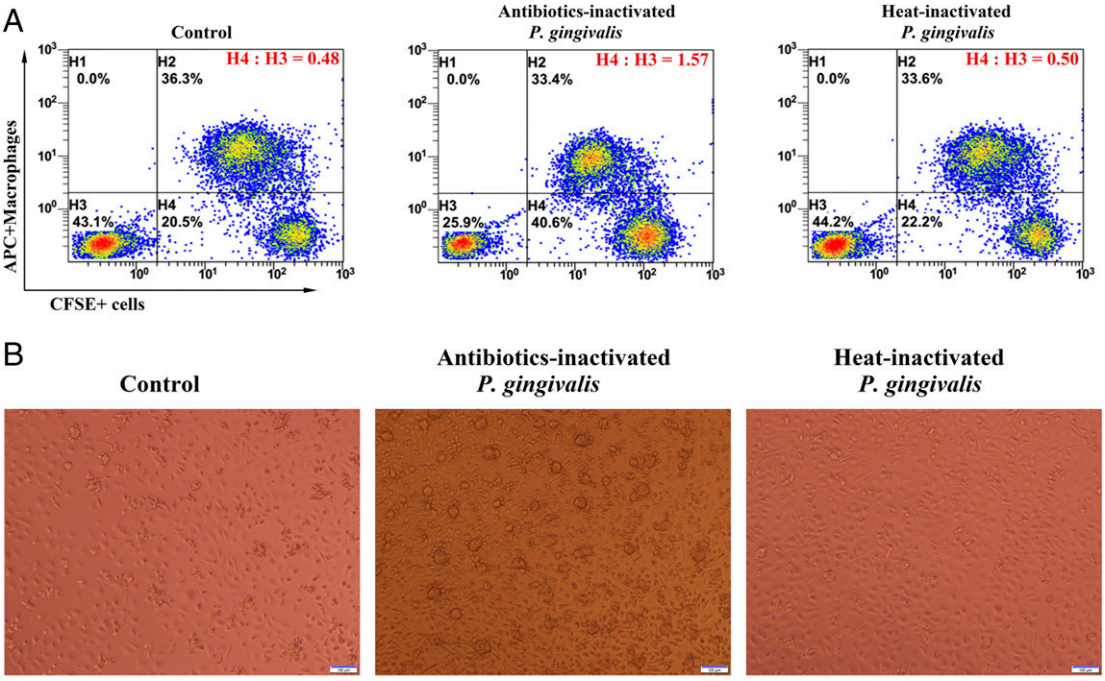

FIGURE 2. Effect of inactivated *P. gingivalis* on macrophages phagocytizing Cal-27 cells overnight. (**A**) Analysis of the proportion of unphagocytized Cal-27 cells by flow cytometry. The ratio of H4 to H3 reflects the relative amount of unphagocytized Cal-27 cells. (**B**) Representative images of the remaining cells after overnight coculture (16 h). Scale bar, 100 μm.

phagocytosis. We studied the effect of *P. gingivalis* on Cal-27 cell–phagocytizing ability of macrophages. For this purpose, we added anti-CD47 Ab to enhance phagocytosis for better observing the function of *P. gingivalis* in mediating phagocytosis of macrophages. The result showed that the proportion of $CFSE^+$ macrophages was decreased with living *P. gingivalis* treatment for 2 h (7.6 versus 11.9%), suggesting a decrease in the proportion of macrophages that had phagocytized Cal-27 cells; this indicated an inhibitory effect of *P. gingivalis* on phagocytosis of Cal-27 cells by macrophages (Fig. 1A). To determine the factor that inhibited phagocytosis (the physiological activity or the membrane-component molecule of *P. gingivalis*), we then used inactivated *P. gingivalis*. We observed that antibiotics-inactivated *P. gingivalis* could also inhibit phagocytosis, and phagocytosis inhibition disappeared when *P. gingivalis* was heated (Fig. 1B), indicating that effector components in *P. gingivalis* would lose function once heated. Therefore, we speculated that membrane-component molecules, such as proteins, functioned to inhibit phagocytosis. To test whether phagocytosis inhibition was specific to *P. gingivalis*, we repeated the phagocytosis experiment with another periodontal pathogen, *Fusobacterium nucleatum* (ATCC 25586). However, *F. nucleatum* failed to inhibit phagocytosis of macrophages (Fig. 1C), suggesting the specific role of *P. gingivalis* in phagocytosis inhibition.

To test whether the phagocytosis inhibition by *P. gingivalis* was a short-term effect, we next cocultured *P. gingivalis* with Cal-27 cells and macrophages overnight (~16 h). In this experiment (Fig. 2A), $CFSE^+$ $F4/80^-$ cells represented unphagocytized Cal-27 cells, and the ratio of unphagocytized Cal-27 cells (H4) to unlabeled cells (H3) reflected the relative amount of unphagocytized Cal-27 cells after an overnight incubation. This ratio was larger in the antibiotics-inactivated *P. gingivalis* group than in the control group (1.57 versus 0.48), which indicated that a higher proportion of unphagocytized Cal-27 cells remained in antibiotics-inactivated *P. gingivalis* group, suggesting the weakened ability of macrophages to phagocytize Cal-27 cells. Fig. 2B showed more cells remained in the bottom of the plate after an overnight incubation with antibiotics-inactivated *P. gingivalis* treatment. No obvious difference was found between the control and heat-inactivated groups. The result showed a trend similar to that of the phagocytosis assay for 2 h.

All phagocytosis experiments were independently repeated thrice (see supplementary material for the results of the three repeated experiments; Supplemental Figs. 2–5).

Sustained infection with P. gingivalis *promoted in vivo OSCC growth*

After demonstrating that *P. gingivalis* protected Cal-27 cells from macrophage attack, next we established a s.c. transplantation model of OSCC in mice and explored the role of *P. gingivalis* in tumor development in vivo. Based on the results from phagocytosis assay, antibiotics-inactivated *P. gingivalis* was used and sustainably injected around tumor sites. As expected, *P. gingivalis*–infected OSCC displayed accelerated growth compared with noninfected OSCC (Fig. 3A). Tumor volume was significantly larger after *P. gingivalis* induction at the treatment points of day 14 and 18. In the current study, the mice were also injected with anti-CD47 Ab, and tumor growth markedly retarded after anti-CD47 injection, irrespective of whether the mice were infected with *P. gingivalis*. These results suggested that *P. gingivalis* promoted in vivo OSCC growth, whereas anti-CD47 inhibited tumor growth.

Sustained infection with P. gingivalis *promoted M2 TAMs polarization*

TAMs are one of the most important components of tumor-infiltrating cells, and they play a major role in tumor immunosurveillance and immunoevasion (23). Macrophages can be classified into M1 and M2 types. M1 macrophages express high levels of MHC molecules and can mediate antitumor immune responses. In contrast, M2 macrophages express low levels of MHC II molecules and are considered to be tumor promotive (22). To explore the role of *P. gingivalis* in the functional polarization of TAMs, we analyzed the composition of TAMs in

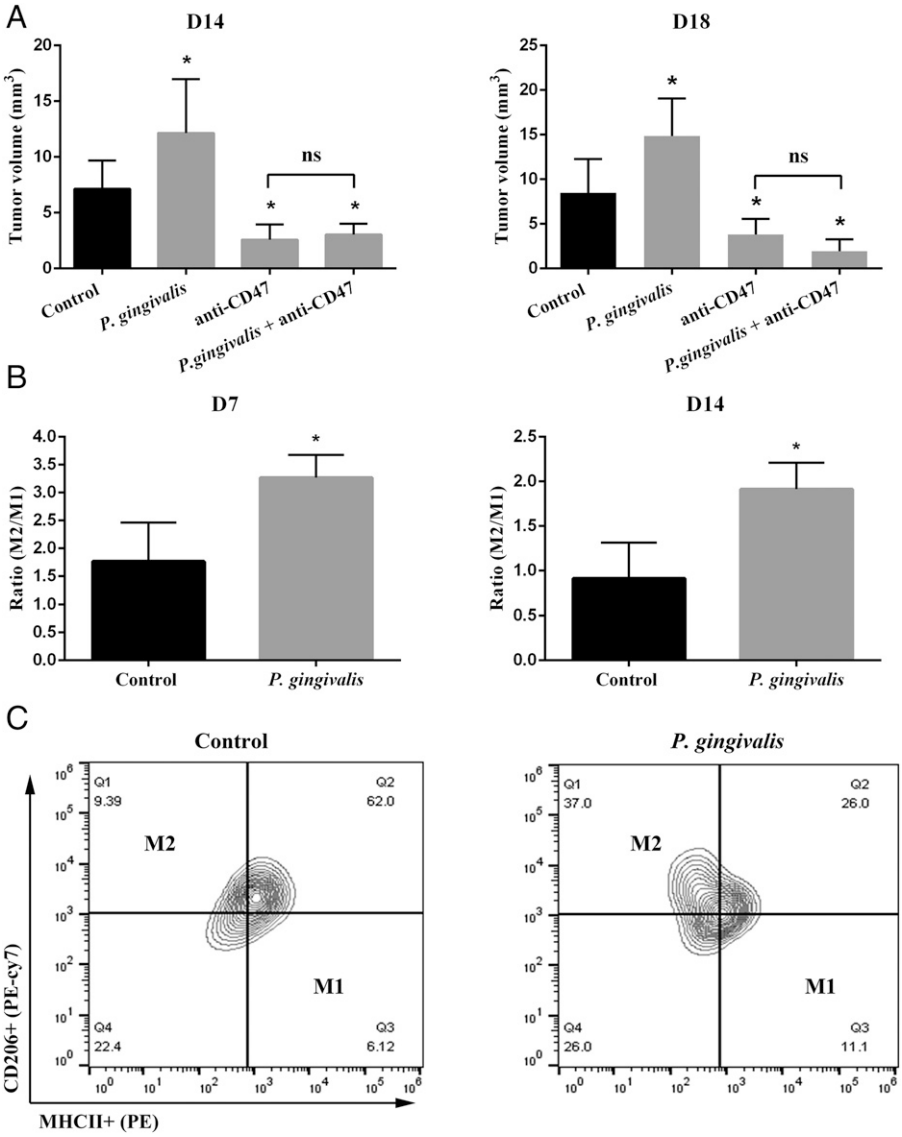

FIGURE 3. Effect of *P. gingivalis* on tumor growth and TAMs polarization in s.c. transplantation of OSCC. (**A**) Tumor volume after treatment with *P. gingivalis* for 14 and 18 d ($n = 6$). (**B**) TAMs polarization analysis after treatment with *P. gingivalis* for 1 and 2 wk ($n = 5$). (**C**) Representative data of analysis of TAMs polarization by flow cytometry. Data are presented as mean + SD, and asterisks represent significant differences compared to the control (physiological saline) group. $*p < 0.05$.

OSCC by flow cytometry. MHC II^+ $CD206^-$ cells were sorted as M1 macrophages, whereas MHC II^- $CD206^+$ cells were sorted as M2 macrophages. The ratio of M2 to M1 macrophages was calculated (Fig. 3B, 3C), and it showed that the M2/M1 ratio was higher in the *P. gingivalis* group than in the control group at both time points, day 7 and 14, indicating that *P. gingivalis* could promote M2 TAMs polarization.

P. gingivalis *upregulated the expression of genes encoding for tumor-promotive molecules in Cal-27 cells and macrophages*

RNA-seq was performed to determine the possible molecular mechanism by which *P. gingivalis* promotes OSCC development. Cal-27 cells or macrophages were stimulated by antibiotics-inactivated *P. gingivalis* and the expression levels of several cytokines were evaluated between infected and noninfected cells. The transcriptome of Cal-27 cells was slightly affected by *P. gingivalis* treatment for 2 h (Fig. 4). Few protumor molecules were upregulated (*IL-1R2*, *suprabasin*, and *TGF-α*) and an antitumor cytokine was downregulated (*TNF-α*). When this stimulation time was prolonged to 16 h, a higher number of protumor molecules (*suprabasin*, *IL-1R2*, *IL-18*, and *TGF-α*) were upregulated, and a higher number of antitumor cytokines (*TNF-β*, *IFN-β*, *TRAIL*, and *TNF-α*) were downregulated. The transcriptome of macrophages was markedly affected by *P. gingivalis* at both time points of 2 and 16 h, with the upregulation of several protumor cytokines (*IL-1α*, *IL-6*, *IL-10*, *IL-18*, *CCL-2*, *CCL-3*, *CCL4*, *CCL-5*, and *CCL7*). To assess the reliability of RNA-seq, we performed qRT-PCR on several selected genes (Cal-27: *cd47*, *il-1r2*, and *suprabasin*; macrophages: *il-1α*, *ccl-3*, and *ccl5*). qRT-PCR showed that *P. gingivalis*–infected Cal-27 cells and macrophages exhibited higher mRNA levels of protumor molecules (*cd47*, *il-1r2*, *suprabasin*, *il-1α*, *ccl-3*, and *ccl5*) than uninfected cells (Fig. 5).

Discussion

A close relationship between microbes and cancer has been reported in many previous studies, indicating that intratumoral microbes can affect cancer growth and metastasis through multiple ways (29). Abundance analysis from clinical samples has revealed that *Porphyromonas* spp. are found at higher levels in intratumoral areas. This result indicates the ability of *Porphyromonas* spp. to invade into tumor interiors, which may help *P. gingivalis* to mediate OSCC growth. Evading immune destruction is a hallmark feature of cancer (21); few studies have focused on the role of *P. gingivalis* in immunoevasion of oral cancer. In the current study, we identified a mechanism by which *P. gingivalis* facilitates

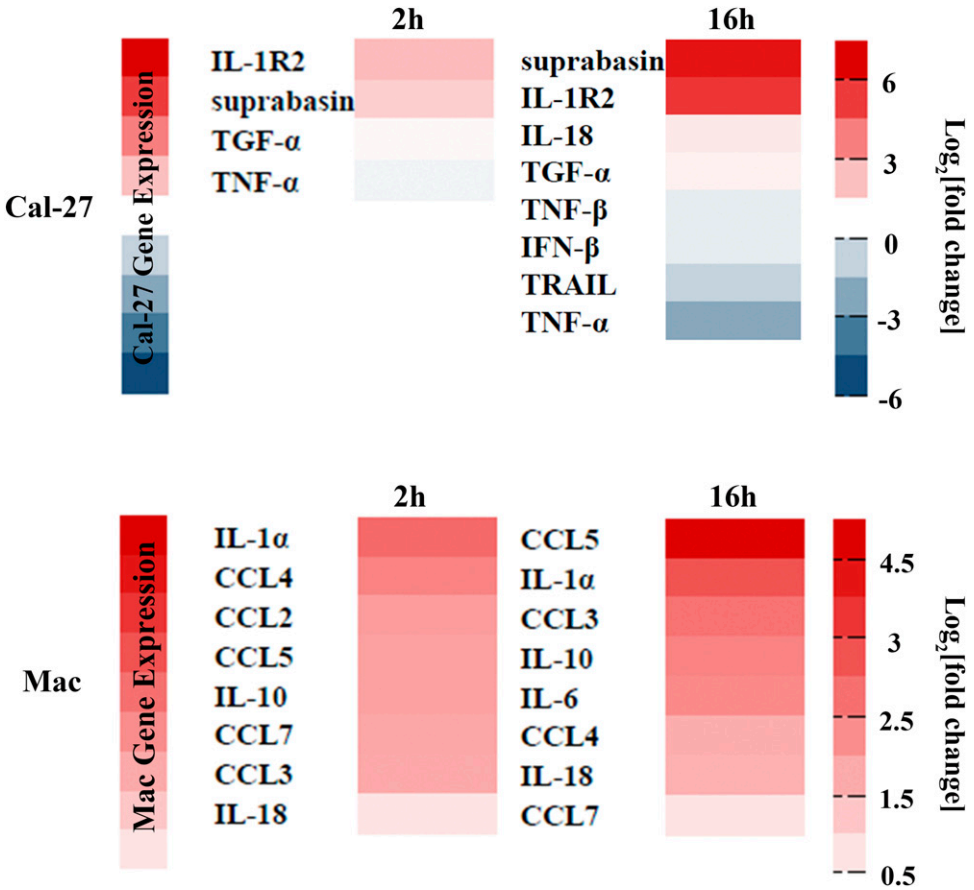

FIGURE 4. Transcriptome analysis of Cal-27 cells and macrophages stimulated by antibiotics-inactivated *P. gingivalis* for 2 and 16 h. Genes listed in the figure are significantly differentially expressed based on p values <0.05.

immunoevasion of OSCC. We report that *P. gingivalis* inhibits macrophages from attacking Cal-27 cells via membrane-component molecules.

Accumulated studies have demonstrated a strong association between *P. gingivalis* and OSCC; *P. gingivalis* was reported to increase the tongue lesion size and multiplicity in a 4NQO-induced oral carcinoma model (30). However to date, the promotive effect of *P. gingivalis* on oral cancer growth has not, to our knowledge, been verified in vivo. Thus, we have found, for the first time to our knowledge, that antibiotics-inactivated *P. gingivalis* infection promoted oral tumor growth in mice. Our result was in line with the observations in the phagocytosis experiment, in which we found that *P. gingivalis* could inhibit macrophages from phagocytizing Cal-27 cells. Macrophages serve as a key mediator in cancer development because inhibition of TAMs attacking is required for the growth and metastasis of solid tumors (24); therefore, we detected the effect of *P. gingivalis* on TAM polarization. Of the two classifications of macrophages, M1 and M2, M1 macrophages express high levels of MHC II, secrete TNF-α, and participate in synthesis of reactive oxygen species and NO. Accordingly, M1 macrophages can efficiently recognize and destroy cancer cells. M2 macrophages, on the contrary, display protumor properties through angiogenesis, tissue remodeling, and suppression of adaptive immunity (31). Thus, the ratio of M2/M1 was evaluated in *P. gingivalis*–infected tumors, to indicate the promotive effect of *P. gingivalis* on M2 TAM polarization; this may be another reason for tumor growth acceleration by *P. gingivalis* infection.

To explore the possible molecular mechanism, we analyzed the transcriptome of Cal-27 cells and macrophages affected by

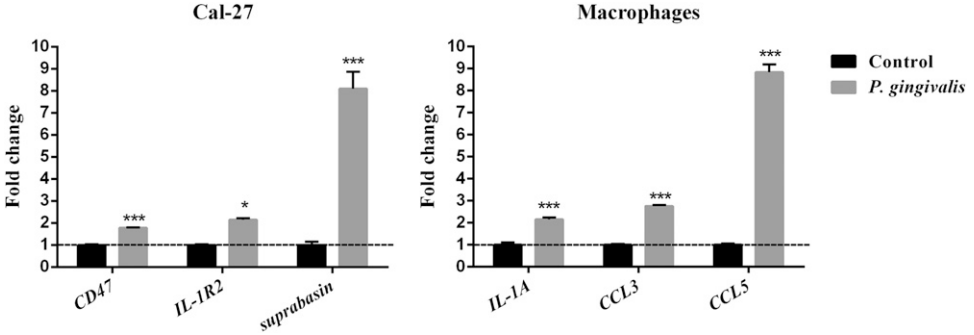

FIGURE 5. Expression of genes in Cal-27 cells and macrophages after stimulation by antibiotics-inactivated *P. gingivalis* for 16 h. Data are presented as mean + SD, and asterisks represent significant differences compared to the control group. *$p < 0.05$; ***$p < 0.001$.

P. gingivalis. According to the results from RNA-seq and qRT-PCR, protumor molecules (including *suprabasin* and *IL-1R2* in Cal-27 cells and *IL-1α*, *CCL-3*, and *CCL-5* in macrophages) were upregulated. Suprabasin has been identified as a tumor endothelial cell marker and may play a role in tumor invasion/metastasis and angiogenesis (32–34). Furthermore, overexpression of *suprabasin* has been associated with the proliferation and tumorigenicity of esophageal squamous cell carcinoma (35). IL-1R2 has been associated with a poor survival rate in colon cancer patients and is correlated with the migration ability of colon cancer cells. IL-1R2 acts with c-Fos to enhance the transcription of IL-6 and VEGF-A, which promotes tumor malignancy and angiogenesis (36, 37). Besides, regorafenib resistance in colon cancer cells is associated with enhanced expression levels of IL-1R2 (38). IL-1α plays roles in the progression of human cervical and breast cancers (39, 40), and is associated with distant metastasis in head and neck squamous cell carcinoma (41). Furthermore, CCL3 might stimulate cancer progression by promoting leukocyte accumulation, tumor growth, and angiogenesis (42). Blockade of CCL3 impairs cell invasion of OSCC and decreases the metastasis of lung cancer and multiple myeloma in mice (42–44). CCL5 can cause changes in the composition of leukocyte cell types at the tumor site by accumulating harmful TAMs (45). CCL5 also can promote tumor invasion, migration, and tumor resistance to host immunosurveillance (46, 47). CCL5 secreted by TAMs may be a novel target in the treatment of gastric cancer (48). Accordingly, the upregulation of these protumor cytokines may be the potential molecular mechanism by which *P. gingivalis* promotes the development of OSCC. However, the specific role of these cytokines in the mediation of OSCC by *P. gingivalis* needs to be confirmed in further studies.

Interestingly, we also found that tumor growth was markedly retarded by anti-CD47 Ab. CD47 is a nonhousekeeping cell surface protein expressed on almost all cancer cells. CD47 functions as a phagocytosis inhibitor by binding to the signal-regulatory protein-α (SIRPα) expressed on phagocytes such as macrophages (49). Therefore, in the in vitro phagocytosis experiment, we added anti-CD47 Ab to enhance the phagocytosis to better observe *P. gingivalis*–mediated phagocytosis. We further found the inhibitory effect of anti-CD47 Ab on OSCC growth in our in vivo study, even under the circumstances of tumor growth promotion by *P. gingivalis*. Weissman et al. (24) pointed out that CD47 might be a therapeutic target for human solid tumors, including ovarian, breast, colon, bladder, and hepatocellular carcinoma and glioblastoma. To our knowledge, our result provided new evidence for anti-CD47 inhibiting human solid tumors. Additionally, we observed that *P. gingivalis* treatment upregulated the expression level of *cd47* in Cal-27 cells. This also can be a candidate mechanism by which *P. gingivalis* promotes OSCC development.

In summary, to our knowledge in this study, we revealed a nove mechanism by which *P. gingivalis* promotes OSCC progression. *P. gingivalis* inhibited the phagocytosis of Cal-27 cells by macrophages, induced functional polarization of macrophages into M2 TAMs, upregulated the expression of genes encoding for protumor molecules in macrophages and Cal-27 cells, and promoted the formation of an immunosuppressive tumor microenvironment, thus triggering immunoevasion of OSCC and promoting OSCC growth. Further studies are needed to identify the effector components in *P. gingivalis*.

Acknowledgments

We thank Min Hu for technical support of flow cytometry.

Disclosures

The authors have no financial conflicts of interest.

References

1. Scully, C., and J. Bagan. 2009. Oral squamous cell carcinoma: overview of current understanding of aetiopathogenesis and clinical implications. *Oral Dis.* 15: 388–399.
2. Bagan, J., G. Sarrion, and Y. Jimenez. 2010. Oral cancer: clinical features. *Oral Oncol.* 46: 414–417.
3. Bray, F., J. Ferlay, I. Soerjomataram, R. L. Siegel, L. A. Torre, and A. Jemal. 2018. Global cancer statistics 2018: GLOBOCAN estimates of incidence and mortality worldwide for 36 cancers in 185 countries. *CA Cancer J. Clin.* 68: 394–424.
4. Torre, L. A., F. Bray, R. L. Siegel, J. Ferlay, J. Lortet-Tieulent, and A. Jemal. 2015. Global cancer statistics, 2012. *CA Cancer J. Clin.* 65: 87–108.
5. Wang, B., S. Zhang, K. Yue, and X. D. Wang. 2013. The recurrence and survival of oral squamous cell carcinoma: a report of 275 cases. *Chin. J. Cancer* 32: 614–618.
6. Vázquez-Mahía, I., J. Seoane, P. Varela-Centelles, I. Tomás, A. Álvarez García, and J. L. López Cedrún. 2012. Predictors for tumor recurrence after primary definitive surgery for oral cancer. *J. Oral Maxillofac. Surg.* 70: 1724–1732.
7. de Moraes, R. C., F. L. Dias, C. M. da Silva Figueredo, and R. G. Fischer. 2016. Association between chronic periodontitis and oral/oropharyngeal cancer. *Braz. Dent. J.* 27: 261–266.
8. Yao, Q. W., D. S. Zhou, H. J. Peng, P. Ji, and D. S. Liu. 2014. Association of periodontal disease with oral cancer: a meta-analysis. *Tumour Biol.* 35: 7073–7077.
9. Moergel, M., P. Kämmerer, A. Kasaj, E. Armouti, A. Alshihri, V. Weyer, and B. Al-Nawas. 2013. Chronic periodontitis and its possible association with oral squamous cell carcinoma - a retrospective case control study. *Head Face Med.* 9: 39.
10. Atanasova, K. R., and O. Yilmaz. 2014. Looking in the *Porphyromonas gingivalis* cabinet of curiosities: the microbium, the host and cancer association. *Mol. Oral Microbiol.* 29: 55–66.
11. Nagy, K. N., I. Sonkodi, I. Szöke, E. Nagy, and H. N. Newman. 1998. The microflora associated with human oral carcinomas. *Oral Oncol.* 34: 304–308.
12. Katz, J., M. D. Onate, K. M. Pauley, I. Bhattacharyya, and S. Cha. 2011. Presence of *Porphyromonas gingivalis* in gingival squamous cell carcinoma. *Int. J. Oral Sci.* 3: 209–215.
13. Yao, L., C. Jermanus, B. Barbetta, C. Choi, P. Verbeke, D. M. Ojcius, and O. Yilmaz. 2010. *Porphyromonas gingivalis* infection sequesters pro-apoptotic Bad through Akt in primary gingival epithelial cells. *Mol. Oral Microbiol.* 25: 89–101.
14. Mao, S., Y. Park, Y. Hasegawa, G. D. Tribble, C. E. James, M. Handfield, M. F. Stavropoulos, O. Yilmaz, and R. J. Lamont. 2007. Intrinsic apoptotic pathways of gingival epithelial cells modulated by *Porphyromonas gingivalis*. *Cell. Microbiol.* 9: 1997–2007.
15. Yilmaz, O., T. Jungas, P. Verbeke, and D. M. Ojcius. 2004. Activation of the phosphatidylinositol 3-kinase/Akt pathway contributes to survival of primary epithelial cells infected with the periodontal pathogen *Porphyromonas gingivalis*. *Infect. Immun.* 72: 3743–3751.
16. Kuboniwa, M., Y. Hasegawa, S. Mao, S. Shizukuishi, A. Amano, R. J. Lamont, and O. Yilmaz. 2008. *P. gingivalis* accelerates gingival epithelial cell progression through the cell cycle. *Microbes Infect.* 10: 122–128.
17. Pan, C., X. Xu, L. Tan, L. Lin, and Y. Pan. 2014. The effects of *Porphyromonas gingivalis* on the cell cycle progression of human gingival epithelial cells. *Oral Dis.* 20: 100–108.
18. Inaba, H., H. Sugita, M. Kuboniwa, S. Iwai, M. Hamada, T. Noda, I. Morisaki, R. J. Lamont, and A. Amano. 2014. *Porphyromonas gingivalis* promotes invasion of oral squamous cell carcinoma through induction of proMMP9 and its activation. *Cell. Microbiol.* 16: 131–145.
19. Perera, M., N. N. Al-Hebshi, D. J. Speicher, I. Perera, and N. W. Johnson. 2016. Emerging role of bacteria in oral carcinogenesis: a review with special reference to perio-pathogenic bacteria. *J. Oral Microbiol.* 8: 32762.
20. Schreiber, R. D., L. J. Old, and M. J. Smyth. 2011. Cancer immunoediting: integrating immunity's roles in cancer suppression and promotion. *Science* 331: 1565–1570.
21. Hanahan, D., and R. A. Weinberg. 2000. The hallmarks of cancer. *Cell* 100: 57–70.
22. Grivennikov, S. I., F. R. Greten, and M. Karin. 2010. Immunity, inflammation, and cancer. *Cell* 140: 883–899.
23. Jaiswal, S., M. P. Chao, R. Majeti, and I. L. Weissman. 2010. Macrophages as mediators of tumor immunosurveillance. *Trends Immunol.* 31: 212–219.
24. Willingham, S. B., J. P. Volkmer, A. J. Gentles, D. Sahoo, P. Dalerba, S. S. Mitra, J. Wang, H. Contreras-Trujillo, R. Martin, J. D. Cohen, et al. 2012. The CD47-signal regulatory protein alpha (SIRPa) interaction is a therapeutic target for human solid tumors. *Proc. Natl. Acad. Sci. USA* 109: 6662–6667.
25. Chao, M. P., R. Majeti, and I. L. Weissman. 2011. Programmed cell removal: a new obstacle in the road to developing cancer. *Nat. Rev. Cancer* 12: 58–67.
26. Pudla, M., C. Srisaowakarn, and P. Utaisincharoen. 2019. NLRP12 negatively modulates inducible nitric oxide synthase (iNOS) expression and tumor necrosis factor-α production in Porphyromonas gingivalis LPS-treated mouse macrophage cell line (RAW264.7). *Inflamm. Res.* 68: 841–844.
27. Hung, S. L., N. G. Lee, L. Y. Chang, Y. T. Chen, and Y. L. Lai. 2014. Stimulatory effects of glucose and *Porphyromonas gingivalis* lipopolysaccharide on the secretion of inflammatory mediators from human macrophages. *J. Periodontol.* 85: 140–149.
28. Holden, J. A., T. J. Attard, K. M. Laughton, A. Mansell, N. M. O'Brien-Simpson, and E. C. Reynolds. 2014. *Porphyromonas gingivalis* lipopolysaccharide weakly

activates M1 and M2 polarized mouse macrophages but induces inflammatory cytokines. *Infect. Immun.* 82: 4190–4203.
29. Garrett, W. S. 2015. Cancer and the microbiota. *Science* 348: 80–86.
30. Wu, J. S., M. Zheng, M. Zhang, X. Pang, L. Li, S. S. Wang, X. Yang, J. B. Wu, Y. J. Tang, Y. L. Tang, and X. H. Liang. 2018. *Porphyromonas gingivalis* promotes 4-nitroquinoline-1-oxide-induced oral carcinogenesis with an alteration of fatty acid metabolism. *Front. Microbiol.* 9: 2081.
31. Rhee, I. 2016. Diverse macrophages polarization in tumor microenvironment. *Arch. Pharm. Res.* 39: 1588–1596.
32. Alam, M. T., H. Nagao-Kitamoto, N. Ohga, K. Akiyama, N. Maishi, T. Kawamoto, N. Shinohara, A. Taketomi, M. Shindoh, Y. Hida, and K. Hida. 2014. Suprabasin as a novel tumor endothelial cell marker. *Cancer Sci.* 105: 1533–1540.
33. Formolo, C. A., R. Williams, H. Gordish-Dressman, T. J. MacDonald, N. H. Lee, and Y. Hathout. 2011. Secretome signature of invasive glioblastoma multiforme. *J. Proteome Res.* 10: 3149–3159.
34. Shao, C., M. Tan, J. A. Bishop, J. Liu, W. Bai, D. A. Gaykalova, T. Ogawa, A. R. Vikani, Y. Agrawal, R. J. Li, et al. 2012. Suprabasin is hypomethylated and associated with metastasis in salivary adenoid cystic carcinoma. *PLoS One* 7: e48582.
35. Zhu, J., G. Wu, Q. Li, H. Gong, J. Song, L. Cao, S. Wu, L. Song, and L. Jiang. 2016. Overexpression of suprabasin is associated with proliferation and tumorigenicity of esophageal squamous cell carcinoma. *Sci. Rep.* 6: 21549.
36. Mar, A. C. 2015. The decoy receptor interleukin-1 receptor type 2 acts as an angiogenic factor in human colorectal cancer. *Cancer Res.* 75: 1361.
37. Mar, A. C., C. H. Chu, H. J. Lee, C. W. Chien, J. J. Cheng, S. H. Yang, J. K. Jiang, and T. C. Lee. 2015. Interleukin-1 receptor type 2 acts with c-Fos to enhance the expression of interleukin-6 and vascular endothelial growth factor A in colon cancer cells and induce angiogenesis. *J. Biol. Chem.* 290: 22212–22224.
38. Mar, A. C., C. H. Chu, C. W. Shiau, and T. C. Lee. 2014. Regorafenib resistance in colorectal carcinoma is associated with enhanced expression of type II interleukin 1 receptor and reversed by MEK/ERK inhibitor. *Eur. J. Cancer* 50: 31.
39. Song, Z., Y. Lin, X. Ye, C. Feng, Y. Lu, G. Yang, and C. Dong. 2016. Expression of IL-1α and IL-6 is associated with progression and prognosis of human cervical cancer. *Med. Sci. Monit.* 22: 4475–4481.
40. Kuan, E. L., and S. F. Ziegler. 2018. A tumor-myeloid cell axis, mediated via the cytokines IL-1α and TSLP, promotes the progression of breast cancer. [Published erratum appears in 2018 *Nat. Immunol.* 19: 1037.] *Nat. Immunol.* 19: 366–374.
41. León, X., C. Bothe, J. García, M. Parreño, S. Alcolea, M. Quer, L. Vila, and M. Camacho. 2015. Expression of IL-1α correlates with distant metastasis in patients with head and neck squamous cell carcinoma. *Oncotarget* 6: 37398–37409.
42. da Silva, J. M., T. P. Moreira Dos Santos, L. M. Sobral, C. M. Queiroz-Junior, M. A. Rachid, A. E. I. Proudfoot, G. P. Garlet, A. C. Batista, M. M. Teixeira, A. M. Leopoldino, et al. 2017. Relevance of CCL3/CCR5 axis in oral carcinogenesis. *Oncotarget* 8: 51024–51036.
43. Wu, Y., Y. Y. Li, K. Matsushima, T. Baba, and N. Mukaida. 2008. CCL3-CCR5 axis regulates intratumoral accumulation of leukocytes and fibroblasts and promotes angiogenesis in murine lung metastasis process. *J. Immunol.* 181: 6384–6393.
44. Coniglio, S. J. 2018. Role of tumor-derived chemokines in osteolytic bone metastasis. *Front. Endocrinol. (Lausanne)* 9: 313.
45. Lv, D., Y. Zhang, H. J. Kim, L. Zhang, and X. Ma. 2013. CCL5 as a potential immunotherapeutic target in triple-negative breast cancer. *Cell. Mol. Immunol.* 10: 303–310.
46. Soria, G., and A. Ben-Baruch. 2008. The inflammatory chemokines CCL2 and CCL5 in breast cancer. *Cancer Lett.* 267: 271–285.
47. Adler, E. P., C. A. Lemken, N. S. Katchen, and R. A. Kurt. 2003. A dual role for tumor-derived chemokine RANTES (CCL5). *Immunol. Lett.* 90: 187–194.
48. Ding, H., L. Zhao, S. Dai, L. Li, F. Wang, and B. Shan. 2016. CCL5 secreted by tumor associated macrophages may be a new target in treatment of gastric cancer. *Biomed. Pharmacother.* 77: 142–149.
49. Chao, M. P., I. L. Weissman, and R. Majeti. 2012. The CD47-SIRPα pathway in cancer immune evasion and potential therapeutic implications. *Curr. Opin. Immunol.* 24: 225–232.